PCP-assisted hydration facilitates robust giant vesicle formation in solutions of physiological ionic strengths

Alexis Cooper[a], Vignesha Vijayananda[b], Joseph Pazzi[b], Anand Bala Subramaniam[b*]

[a] Department of Chemistry and Biochemistry, University of California, Merced, Merced, CA 95343, United States.

[b] Department of Bioengineering, University of California, Merced, Merced, CA 95343, United States.

*Email: asubramaniam@ucmerced.edu

Abstract

Achieving efficient assembly of giant unilamellar vesicles (GUVs) in solutions of physiological ionic strength remains a major challenge due to lipid membrane adhesion, which inhibits the formation of buds and foam-like mesophases. While osmotic pressure from partially soluble polymer films can balance the adhesion between membranes, dewetting of the polymer film upon hydration significantly limits GUV formation, particularly at elevated temperatures. Here, we develop polymer-coated nanocellulose paper (PCP) as a nanostructured substrate that overcomes dewetting limitations, enabling the use of highly soluble polymers to exert osmotic pressure. Hydration of thin lipid films on PCP, PCP-assisted hydration, facilitates robust GUV formation in salty solutions across a broad temperature range (4 °C to 45 °C) with diverse polymers, including ultralow-gelling agarose, hyaluronic acid, dextran, carrageenan, and polylysine. Furthermore, we demonstrate that PCP-assisted hydration simplifies encapsulation of complex biochemical mixtures, supporting for example, cell-free protein expression and actin ring formation within GUVs. PCP-assisted hydration enables scalable production of over 10^9 GUVs in physiologically relevant buffers, providing a high-throughput and versatile platform for applications in synthetic biology, drug delivery, and biophysics.

1. Introduction

Self-assembly of lipid films in low salt aqueous solutions into surface-attached micrometer-sized buds or volume-spanning "foam"-like mesophases is a precursor to the formation of cell-sized giant unilamellar vesicles (GUVs) via thin film hydration methods.[1,2] The GUV molar yield, *Y,* which is the amount of lipids in the membranes of the harvested GUVs relative to the amount of lipids deposited on the surface, reported as a percentage, was recently proposed to allow comparison between different conditions of assembly. The molar yield of GUVs is akin to the yield used in chemical synthesis, the reactant is the amount of lipid on the surface, and the product is the amount of lipid that ends up in the membranes of the GUVs. Qualitative categories classify the quantitative numbers into relative ranges, "negligible", $Y < 1$ % "low", $1 \leq Y < 10$%, "moderate", $10 \leq Y < 20$ %, "high", $20 \leq Y < 45$ % and "ultrahigh", $Y \geq 45$ %.

GUV yields obtained using thin film hydration methods, such as gentle hydration on glass slides, PAPYRUS, and electroformation were moderate or high when performed using low salt solutions.[3] However, in salty solutions, including those of physiological ionic strengths, the increased adhesion between the lamellar bilayers prevents the formation of buds on the surface or the formation of foam-like mesophases resulting in negligible yields of GUVs.[2] While GUVs encapsulating low salt solutions have myriad uses in biophysical and biological applications,[4–9] reconstitution of cellular proteins often requires a salty interior[10–17] marking a significant limitation to thin film hydration techniques. Depositing a dry film of partially soluble polymers such as agarose of various gelling temperatures or polyvinyl alcohol (PVA) onto glass slides prior to depositing the lipid allows the formation of GUVs in salty solutions.[18–20] The polymer films partially dissolve and exert an osmotic pressure against the stacks of membranes which overcomes the increased adhesion between the lipid bilayers.[18,20] GUV yields mostly ranged from low to

moderate. The highest measured yield, ~ 17 %, was only achieved for low gelling temperature (LGT) agarose at 22 °C. [20] Agaroses of all other melting temperatures and polyvinyl alcohol (PVA) had yields below 10 %. LGT agarose at temperatures other than 22 °C had yields of < 5 %. Polymers such as medium and high melting temperature agarose and PVA had insufficient dissolution, while polymers such as ULGT agarose at 22 °C and both LGT agarose and ULGT agarose at elevated temperatures experienced dewetting on the glass substrate. Insufficient dissolution and extensive dewetting both result in low yields and GUVs of small diameters upon harvesting.[20]

Here, we seek to address these limitations. We hypothesize that suppression of polymer dewetting from the substrate will allow the use of soluble polymers to obtain GUV yields of > 15 % in salty solutions. We test this hypothesis by considering the physicochemical causes of dewetting. We then address the causes by using a natural nanostructured material, nanocellulose paper, as a substrate, and by controlling the surface concentration of the polymer to create Polymer-Coated nanocellulose Paper (PCP). We find that with dewetting suppressed, a wide variety of soluble macromolecules, including biocompatible and biomedically-relevant polymers such as hyaluronic acid, dextran, carrageenan, and polylysine, can be used to obtain GUV yields of > 15 % in salty solutions at a variety of temperatures by hydrating the lipid films on PCP (PCP-assisted hydration). We demonstrate that the PCP-assisted hydration technique effectively prepares GUVs that encapsulate functional complex biochemical mixtures such as commercial cell-free protein expression systems and G-actin and the bundling protein fascin. The first achieves ~100% deGFP expression from deGFP plasmids and the second forms single actin rings within the assembled GUVs. PCP-assisted hydration is highly adaptable, generating GUVs from PCP pieces as small as 3 mm in diameter with 12 μL of buffer to sheets as large as 279 mm × 178 mm in 200 mL of buffer.

Under the latter conditions, the method produces approximately 6×10^9 GUVs that encapsulate physiological saline.

2. Results and Discussion

We first consider the evolution of a surface-attached film composed of partially soluble polymers in the context of assembling GUVs. The polymer film on the surface is prepared by spreading an aqueous polymer solution. Drying of the aqueous polymer solution results in the formation of an amorphous glassy polymer film on the substrate. Lipids dissolved in a volatile organic solvent are then deposited onto the polymer film. The solvent evaporates leaving a dry film of lipids. Upon hydration, the dry lipids self-assemble to form stacks of lamellar lipid bilayers, and water diffuses into the amorphous polymer layer, forming a gel-like swollen layer. The swelling causes an increase in mechanical stress in the polymer layer. The stress can be relieved when the polymer molecules dissolve by disentangling and diffusing into the solvent.[21] Polymer dissolution is the desired outcome for exerting osmotic pressure against the lamellar bilayers to form GUV buds. However, when the adhesion of the polymer film to the substrate is poor, the stress can be relieved by dewetting the polymer film and the attached lamellar bilayers to form hybrid polymer-lipid "pseudobuds" instead of GUV buds.[20]

We reasoned that three material factors could reduce dewetting while preserving the ability of the polymer to dissolve and exert osmotic pressure on the lamellar bilayers: 1) A nanostructured surface could help prevent dewetting by providing pinning sites and breaking the polymer film into islands to provide gaps which could relieve swelling stresses prior to dissolution. 2) Surfaces with similar surface chemistry to the polymers could promote the wetting and adhesion of the solvent swollen polymer layer. 3) Low concentration of polymers to form thin films of polymers could reduce any transient mechanical stress anisotropy.

To test these three material factors, we choose nanocellulose paper as our model rough nanostructured substrate (Figure 1a, inset).[3] Unlike glass which is smooth (Figure 1b, inset), nanocellulose paper is composed of polydisperse entangled cylindrical fibers ~ 17 nm in radius and ~ 2 μm in length.[3] Cellulose is an insoluble polysaccharide with many terminal hydroxyl groups and shares similar surface chemistry to water-soluble polymers.[22,23] Cellulose, although insoluble in water, swells in water, thus potentially matching the rate of swelling of the polymer and reducing the mechanical anisotropy between the polymer and substrate interface. Furthermore, although paper composed wholly of nanocellulose can be made from nanocellulose pulp, a substrate with a surface layer of densely-packed nanocellulose fibers can be obtained commercially at very low cost in the form of acid-free artist grade tracing paper.[3] For the purposes of assembling GUVs, these two substrates are indistinguishable.[3] We thus refer to tracing paper as nanocellulose paper in this work.

To test simultaneously the effects of the surface concentration of the polymer and the identity of substrate on the assembly of GUVs, we use the polymer ultralow gelling temperature (ULGT) agarose to create polymer-coated nanocellulose paper (PCP) and polymer-coated glass (PCG) substrates. ULGT agarose which has a higher solubility than agaroses of higher melting temperatures dewets from glass coverslips when used to assist the assembly of GUVs resulting in yields of < 2 %.[20] We prepared ULGT agarose PCP and PCG substrates with polymer nominal surface concentration (polymer-NSC) of 0, 0.05, 0.5, 1.5, and 5.2 nmol/cm^2, deposit 10 μg of 1,2-dioleoyl-*sn*-glycero-3-phosphocholine (DOPC) with 3 mol % of 1,2-dioleoyl-*sn*-glycero-3-phosphoethanolamine-*N*-[methoxy(polyethylene glycol)-2000] (ammonium salt) (PEG2000-DSPE) and 0.5 mol % TopFluor™ Cholesterol (TopFluor™ Chol), and allow the assembly to proceed for 1 hour in phosphate buffered saline (PBS). We report in Supporting Text and Table S1

the polymer-NSC of agarose and PVA that have been used in the literature. The addition of 3 mol % of PEG2000-DSPE to the lipid mixture provides steric repulsion between the membranes and prevents aggregation of the GUV buds and GUVs in salty solutions (Figure S1). TopFluor™ Chol allowed visualization of the membranes with confocal microscopy.

To obtain GUVs, we use a pipette to apply fluid shear to harvest any buds that formed on the substrates. We quantified the distribution of diameters and counts and then calculated the molar yield of the GUVs via previously established image analysis procedures (Figure 1a,b).[3,20] We show representative images of the harvested objects and histograms of the diameter distributions of the GUVs obtained using the ULGT agarose PCP and PCG in Figure S2 and S3 respectively. We find that the yield of GUVs evolved non-monotonically with the polymer-NSC for both the ULGT agarose PCP and PCG substrates. This result shows the multivariate effect of substrate identity and the polymer-NSC on the assembly of GUVs. As expected, absent any ULGT agarose, the molar yield was negligible, < 1 %, for both substrates. Furthermore, there were hardly any lipid structures, i.e. GUVs, multilamellar vesicles (MLVs) or lipid debris in the solution, indicating that most of the lipids remained on the surfaces (Figure S2a,f). For both surfaces, the yield increased before reaching a peak and then decreased with an increase in the polymer-NSC. The peak yield obtained using ULGT agarose PCG was 10.2 ± 0.8 % and was obtained at a polymer-NSC of 0.5 nmol/cm^2. The peak yield obtained using ULGT agarose PCP was double that of the ULGT agarose PCG at 21.1 ± 1.0 % and was obtained at a polymer-NSC of 1.5 nmol/cm^2. We term the polymer-NSC that produces the peak yield as the "optimal polymer-NSC". A polymer-NSC of 5.2 nmol/cm^2 resulted in a decrease in the molar yield to 1.6 ± 0.5 and 13.3 ± 0.9 % for both ULGT agarose PCG and PCP respectively. For all the polymer-NSCs tested, ULGT agarose PCP had a higher molar yield than ULGT agarose PCG. These differences in yield have practical consequences. Figure

1c,d show that the number of GUVs with diameters > 10 μm was strongly linearly correlated with the molar yield of GUVs (Figure 1c, Pearson's R=0.9933; Figure 1d, Pearson's R=0.9607). This result demonstrates that obtaining GUVs desired for most biophysical experiments, that is, GUVs > 10 μm, use of substrates that produce high molar yields is advantageous. Additionally, a fortuitous observation was that the samples obtained from PCP-assisted hydration had consistently lower amounts of non-GUV structures in the solution compared to the samples obtained from PCG-assisted hydration (Figure 1e,f, white arrows, see Figure S2 for additional images). For example, even when the molar yields of GUVs were similar ~ 10 %, the percentage of non-GUV structures from PCG-assisted hydration was more than double that of PCP-assisted hydration, 19.4 ± 0.6 % versus 8.5 ± 0.3 % respectively (see Figure S3 for percentage of non-GUV structures for the other polymer-NSCs).

To understand the non-monotonic evolution of the GUV yields and the lower amount of lipid debris from PCP-assisted hydration compared to PCG-assisted hydration, we obtained images of the lipid film on the surfaces prior to harvesting. We find that the PCP and PCG surfaces were covered with varying fractions of lamellar bilayer stacks, GUV buds, and hybrid lipid-polymer pseudobuds (Figure 2). Lamellar bilayer stacks appeared as flat fluorescent regions (yellow arrows), GUV buds appear spherical with uniform intensity (white arrows), and hybrid lipid-polymer pseudobuds have micrometer-sized non-fluorescent dark regions at their base (red arrows). No foam-like mesophase was apparent in any of these images. When harvested, the GUV buds self-close to form GUVs and the lipid-polymer pseudobuds form MLVs and other lipid debris.[20] There were large areas of lipid bilayer stacks without any buds on both surfaces at the lowest polymer-NSC of 0.05 nmol/cm^2 (Figure 2a,b, yellow arrows). We interpret that these regions did not have sufficient polymer to dissolve to overcome the increased adhesion of the

bilayers in PBS. At the optimal polymer-NSC the surfaces had a high fraction of GUV buds. The ULGT agarose PCP had a larger number of GUV buds and a lower fraction of pseudobuds compared to the ULGT agarose PCG (Figure 2c,d). At polymer-NSC higher than the optimal polymer-NSC, both surfaces had large numbers of pseudobuds and large non-fluorescent dark areas (Figure 2e,f). The dark areas are indicative of dewetting and lift-off of the fluorescent lipid and polymer film. We conclude that both the surface topography of the nanocellulose paper and the low polymer-NSCs effectively suppresses polymer dewetting and reduces the formation of lipid-polymer pseudobuds. The suppression of dewetting increases GUV yields in salty solutions. Additionally, the reduced formation of lipid-polymer pseudobuds on the nanocellulose paper surface explains the reduced amount of lipid debris and MLVs from ULGT agarose PCP relative to PCG.

Having shown that nanocellulose paper suppresses polymer dewetting, increases yields, and decreases lipid debris, we next test the performance of PCP-assisted hydration at different temperatures. GUVs must be assembled at temperatures above the chain melting temperature of the constituent lipids. For lipid mixtures, the assembly temperature must be above the lipid with the highest chain melting temperature.[24] Previously, we found that assembly at temperatures of ≥ 37 °C resulted in a greatly reduced yield of GUVs using LGT and ULGT agarose-coated glass coverslips.[20] High temperatures increased the solubility of the polymer, resulting in the temperature-induced dewetting of the polymer film from the glass surface. We perform PCP-assisted hydration using a canonical ternary lipid mixture that exhibits "raft" phases at room temperature. The mixture consists of DOPC:1,2-dipalmitoyl-*sn*-glycero-3-phosphocholine (DPPC):Cholesterol:DSPE-PEG2000:1,2-dioleoyl-*sn*-glycero-3-phosphoethanolamine-*N*-(lissamine rhodamine B sulfonyl) (ammonium salt) (Rhod-DOPE): TopFluor™ Chol at a mol % of

36:33:27.5:3:0.25:0.25. The membranes of the GUVs are expected to phase separate into equal area fractions of a DOPC-enriched liquid disordered (L_d) phase and a DPPC and cholesterol enriched liquid ordered (L_o) phase when quenched to room temperature.[24] The Rhod-DOPE partitions into the L_d phase while the TopFluor™ Chol partitions into the L_o phase, allowing visualization of these phases in the membranes of the GUVs. The chain melting temperature of DPPC is 41.5 °C [23] and thus we performed PCP-assisted hydration at 45 °C.[24] The yield of the phase-separating GUVs was 17.0 ± 2.7 % after 1 hour which was statistically indistinguishable from the yield of single phase DOPC GUVs obtained using PCP-assisted hydration at 22 ºC (p = 0.118) (Figure 3a). We investigated the effect of incubation time on PCP-assisted hydration since high temperatures lead to time-dependent denaturation of proteins.[25] At 45 ºC, a short 20-minute incubation preserves the functionality of membrane proteins such as human serotonin receptor 5-HT_{1A} which otherwise denatured when incubated for long periods.[25] The yield of the phase-separating GUVs obtained using PCP-assisted hydration was 11.2 ± 0.6 % after 20 minutes of incubation. This yield was more than 3× higher than the 3.2 ± 1.0 % yield of phase-separating GUVs that was obtained using PCG-assisted hydration under similar conditions (Figure 3b). Furthermore, the phase-separating GUVs had equal area fractions of L_d and L_o phases (Figure 3c). This result shows that PCP-assisted hydration is similar to other thin film hydration methods that are known to produce GUVs with compositions that largely reflect the composition of the lipid stock.[26]

In addition to higher than room temperature assembly, GUVs are often assembled at low temperatures, 4 °C, to prevent premature reaction when constructing synthetic cells.[10,13,14] For future cold-chain biomedical applications, assembly and storage of GUVs at low temperature could be useful for reducing the rate of activity of degradative enzymes, the rate of growth of

microorganisms, and the rate of intrinsic degradation of biomolecules.[27,28] We perform PCP-assisted hydration at 4 °C using DOPC. We use DOPC since its chain melting transition temperature is – 17 °C.[29] We obtained a yield of 22.3 ± 2.0 % (Figure 3d). This yield was statistically indistinguishable from the yield obtained from PCP-assisted hydration at room temperature (p = 0.499). We show a representative image and histograms of the diameter distributions in Figure S4 and S5. We conclude that by suppressing dewetting, PCP-assisted hydration supports the efficient assembly of GUVs of various membrane compositions at a variety of temperatures and incubation times.

Assembly of GUVs using assisting compounds necessarily leads to the incorporation of the compounds in the resulting GUVs.[20,30,31] Since the incorporation of polymers is a necessary feature of the technique, we explored if there are limits to the identity of the polymer. Thus far, extant reports use partially-soluble[18,19] or cross-linked polymers[32,33] on smooth glass surfaces, overwhelmingly ultra-low gelling temperature agarose or PVA. We choose from a selection of highly soluble polymers with known biomedical applications[34–43] to provide the greatest contrast with extant reports. We use three polysaccharides, hyaluronic acid, dextran, and carrageenan, and a polypeptide, poly-D-lysine. Hyaluronic acid (HA) is an anionic polymer used in wound healing, in tissue engineering, and in cosmetics.[35] Dextran is a clinically-approved plasma expander[36] and a contrast agent for magnetic resonance imaging.[37] When chemically cross-linked, dextran hydrogels are used in tissue engineering applications.[38,39] Carrageenan is a gel-forming polymer used as scaffolds in tissue engineering,[42] in drug delivery applications,[41,43] and in food to modify viscosity and texture.[41] Polylysine is used extensively as a promoter for cell adhesion in cell-culture.[40] We used hyaluronic acid of two different molecular weights (MW), 8-15 kDa and 70-120 kDa, dextran with a MW of 100 kDa, carrageenan with a MW of 521 kDa, and poly-D-lysine

with a MW of 70-150 kDa. We also tested fragmented salmon DNA that was ~ 587- 837 base pairs with a MW of 274kDa and bovine serum albumin (BSA) with a MW of 66 kDa. These two compounds are not used for biomedical applications but have different macromolecular and chemical characteristics compared to the other polymers that we tested. Salmon DNA is a nucleic acid and BSA is a globular protein. We screened various surface concentrations and assembly conditions (See Methods) and report in Table 1 the polymer-NSC that corresponded to the highest GUV yield. We additionally tabulate the counts of GUVs and the percentage of non-GUV structures.

We find that most of these molecules support the formation of GUVs at moderate to high yields via the PCP-assisted hydration technique, 13 - 22 %, at the various temperatures of assembly that we tested. Use of hyaluronic acid PCP to assemble GUVs results in high yields of 20.4 ± 0.9 %, 22.0 ± 2.5 %, and 17.5 ± 2.2 % at 4 °C, 22 °C, and 45 °C respectively. Use of dextran PCP to assemble GUVs resulted in yields of 17.7 ± 0.7 % and 15.0 ± 0.3 % at 4 °C and 22 °C. Use of poly-D-lysine PCP to assemble GUVs resulted in a high yield of 18.6 ± 3.0 % at 22 °C. Use of nanocellulose paper as a substrate was essential for obtaining high yields of GUVs using these highly soluble polymers. Use of glass as a substrate resulted in massive dewetting of the lipid-coated polymer films and negligible yield of GUVs (Figure S6). While performing PCP-assisted hydration using DNA and BSA resulted in higher yields compared to using bare nanocellulose paper, the yields of GUVs were low, 6.7 ± 1.2 % and 6.1 ± 0.5 % respectively.

We find no general correlation between the molecular weight and optimal polymer-NSC with the yields of GUVs obtained from PCP-assisted hydration (Table 1). This observation is consistent with more than one process, interactions with the membrane, dewetting, and solubility affecting the yield.[20] Thus, the polymer-NSC must be optimized for each novel macromolecule

when fabricating PCP for use in PCP-assisted hydration. We show additional results and discussion from our screen of various polymer types, polymer-NSC, and temperatures in Supplementary Text and Tables S2-S5.

Since obtaining GUVs in salty solutions is desired to reconstitute biochemical reactions within cell-like confines and to assemble synthetic cells, we tested the ability of PCP-assisted hydration to functionally encapsulate two "difficult" biochemical reactions, cell-free transcription translation (TXTL) expression of proteins from a nucleic acid template[13] and the reconstitution of actin bundles. Commercial cell-free expression platforms are proprietary mixtures of high concentrations of proteins, salts, and other promoters. Reconstitution of actin bundles requires the encapsulation of G-actin and bundling proteins in monomeric form prior to actin polymerization and bundling in GUVs.[10–12]

We perform PCP-assisted hydration using commercial cell-free protein expression mixture (myTXTL® Pro) with 5 nM (13.4 ng/μL) of T7 deGFP plasmid. Successful expression of the plasmid results in the formation of green fluorescent protein (GFP) which can be imaged with fluorescence microscopy. We cut the PCP into a 3 mm diameter disk to scale down our typical assembly volume by 12.5× to the 12 μL volume recommended by the manufacturer. We use 0.5-mL PCR tubes for fluid management (Figure 4a). We perform PCP-assisted hydration at 4 °C. The low temperature prevents the premature expression of deGFP.[13] After 1 hour, we harvested the GUV buds to obtain GUVs and then incubated the suspension at room temperature for 6 hours to allow gene expression. We then imaged the GUVs using dual-channel confocal microscopy. Figure 4b shows representative images of the harvested GUVs. The method resulted in ~ 1×10^5 GUVs in the chamber. Figure 4c shows a histogram of the luminal intensity of n = 660 GUVs (green bars). We show the results of a second independent repeat in Figure S7. The mean intensity in the

lumens was 25 ± 8 arbitrary units (AU), and the lowest measured intensity was 5.5 AU. In contrast, the mean intensity of a control that was prepared and imaged identically but with plasmid omitted was 3 ± 1 AU. The highest measured luminal intensity was 5 AU (Figure 4c, white bars). We conclude that 100% of the GUVs prepared with the T7 deGFP plasmid had measurable gene expression. 98% of GUVs had measurable gene expression in the second independent sample (Figure S7). Previous reports encapsulating commercial PURE systems using the emulsion transfer technique with 10 ng/μL of template DNA resulted in 87 % of the GUVs having measurable GFP expression[13] and a bead-based freeze-thaw technique with 7.4 nM template DNA resulted in 30 % of the GUVs having measurable yellow fluorescent protein (YFP) expression.[14] An additional parameter that is often measured is the coefficient of variation (CV), which reflects the variation in the concentration of the expressed protein in the population of GUVs. Reported CVs of GFP intensity for the inverted emulsion technique is between 0.3 and 0.5.[15,16] The CV for YFP intensity expressed in the lumens of the GUVs from the bead-based freeze thaw technique was not reported. We obtained a CV of 0.30 for the sample shown in Figure 4 and a CV of 0.31 in Figure S7. We conclude that PCP-assisted hydration is effective at obtaining hundreds of thousands of GUVs with high expression levels and low CV while using minute quantities of the cell-free expression mixture.

We next evaluated the effectiveness of the PCP-assisted hydration technique for obtaining actin bundles in GUVs. We encapsulate 12 μM actin with 1.8 μM fascin in actin polymerization buffer with the goal of forming actin rings. We use a 12 μL reaction volume and perform PCP-assisted hydration at 4 °C to reduce the premature polymerization of G-actin into F-actin during the encapsulation process.[10] We acquired confocal Z-stacks and projected the three-dimensional stacks into two-dimensional images using the “maximal intensity projection” method in ImageJ.

We obtain GUVs that ranged in diameters from 2 μm to 20 μm. We limited our analysis to GUVs that had diameters ≥ 6.5 μm since it was difficult to discern the thin actin bundles in small GUVs. We find that 74% of GUVs had actin bundles in their lumens and that the presence of actin bundles did not depend on the diameter of the GUVs (n = 68 total GUVs counted, Figure S8). Movement of the GUVs during Z-stack acquisition and the relatively low resolution of the 20× 1.0 NA Plan Apochromat objective that we used made it difficult to discern the morphology of the actin bundles that were present in the GUVs. We thus prepared a second independent sample, immobilized the GUVs onto the surface of a glass coverslip, and obtained superresolution images of the actin bundles in the GUVs (Figure 5d-e). We find that 87% of the GUVs had actin bundles in their lumens and the presence of actin bundles did not depend on the size of the GUVs (n=53 total GUVs counted, Figure 5f). 26 % of the GUVs had single actin rings, 54 % of the GUVs had single actin rings that were not closed or had one or more branches, and 20 % of the GUVs had multiple actin rings that consisted of single actin rings or rings with branches (n=46 GUVs with actin bundles). Examples of GUVs encapsulating these structures are shown in Figure S9. This result is comparable to encapsulating actin and fascin using the emulsion transfer technique, where the authors found that 12 % of the GUVs had single actin rings.[12] We estimate that there were ~ 1×10^4 GUVs with actin bundles in the chamber. Furthermore, as expected, increasing the actin concentration resulted in GUVs with network-like actin bundles and protrusions (Figure S10).[10]

In addition to scaling down to work with small volumes of precious samples, PCP-assisted hydration can also be scaled up to obtain large numbers of GUVs by using large pieces of PCP. We show an example of a protocol that can be performed in a typical laboratory using a 330 mm × 279 mm (13-in. × 11-in) commercial baking tray as a fluid receptacle and a piece of paper 279 mm × 178 mm (11-in × 7-in). For this experiment, we use dextran PCP since dextran has a lower

cost compared to the other polymers (Table S6). We obtain 188 mL of suspension containing a total of 5.5×10^9 GUVs in a single preparation (Figure 5a). The histogram of sizes is shown in Figure S11. The number of GUVs obtained is 1344× higher than a single well in a 48-well plate and 28× higher if hypothetically all 48-wells were used (Figure 5b). We create an artificial tissue-like structure with the GUV suspension. Figure 5c shows a 300 μm × 300 μm two-dimensional Z-coded projection of a tissue-like layer with a length × width × height of 5900 μm × 5900 μm × 24 μm. The tissue-like layer was obtained by pelleting the GUVs from 7.5 mL of the GUV suspension via centrifugation and then taking a 30 μL of the pellet and allowing the GUVs to sediment in an imaging chamber for 3 hours (See Experimental Section for full details). We thus could obtain ~ 25 of these tissue-like layers from a single preparation. Notably, although the whole preparation took a relatively short 2.5 hours after the PCP was prepared, active user engagement was only ~ 30 minutes during the spreading of the lipid, pouring of the hydration buffer, and harvesting of the GUVs. The additional two hours were for solvent evaporation (1 hour) and incubation in the buffer (1 h). Due to the short user engagement time, the method could be easily parallelized with multiple sheets of paper and baking trays.

Since preparation of the PCP required the longest time in the protocol, ~ 4 hours, we investigated how long a piece of ULGT agarose PCP could be used after fabrication. We find that PCP stored on a room temperature laboratory bench can be used for up to 21 days without significant loss of GUV yield or apparent reduction in the quality of GUVs with storage time (Figure 5d-e). After 28 days of storage, the yield falls significantly to 11.0 ± 0.7 %. The GUVs that were harvested however appeared identical to those obtained at earlier times. Storing the paper at 4 °C prevented this apparently slow degradation of the properties of the PCP. There was no reduction in yield when the paper was retrieved from the refrigerator after 28 days. However,

repeated removal of the PCP from the refrigerator should be avoided since it results in condensation which decreases the yield with each removal (Figure S12).

3. Conclusion

In summary, we demonstrate that nanocellulose paper as a substrate significantly expands the range of polymers that can facilitate the assembly of GUVs in salty solutions, enabling the use of at least six soluble macromolecules: hyaluronic acid, dextran, carrageenan, poly-D-lysine, BSA, and DNA. By preventing dewetting, PCP ensures high GUV yields across a wide range of assisting macromolecules and maintains robust assembly across temperatures from 4 °C to at least 45 °C. Additionally, PCP-assisted hydration offers practical advantages: large sheets can be prepared within hours for bulk GUV assembly in hundreds of milliliters of buffers or tailored for small-scale use in well plates and PCR tubes. The prepared paper remains stable for at least 21 days, providing flexibility for experimental workflows. We anticipate that PCP-assisted hydration, with the polymer selection reported here and potentially others yet to be explored, will serve as a valuable tool for assembling GUVs in salty solutions, advancing biophysical and biomedical applications.

4. Experimental Section

Materials

We purchased premium plain glass microscope slides (75 mm × 25 mm), 48-well polystyrene tissue culture plates (Fisherbrand), Fisherbrand™ Ultra-Clean™ Supreme Aluminum Foil, glass coverslips (Corning, 22 mm × 22 mm), Falcon™ Bacteriological Petri Dishes with Lid, 2 mL disposable glass Pasteur pipettes, dropper bulb, 4 mL glass vials, 50 mL Falcon centrifuge tubes, and Eisco™ Mixed Set of Glass Delivery Tubes from Thermo Fisher Scientific (Waltham, MA). We purchased Grafix shrink film (8.5-in × 11-in) and a 330 mm × 279 mm (13-in. × 11-in.) baking tray (Wilton) from Amazon.com (Seattle, WA, USA). We purchased acid-free artist grade tracing paper (Jack Richeson and Co. Inc) from an online vendor Brushes and More.

Chemicals

We purchased sucrose (BioXtra grade, purity ≥ 99.5%), glucose (BioXtra grade, purity ≥ 99.5%), casein from bovine milk (BioReagent grade), agarose type IX-A: ultra-low gelling temperature (Catalog number: A2576, molecular biology grade), agarose: low gelling point (Catalog number: A9414, molecular biology grade), deoxyribonucleic acid, single stranded from salmon testes (D7656), carrageenan (C1013), dextran from *Leuconostoc spp*. (Catalog number: 09184, MW: 100,000), bovine serum albumin (Catalog number: A3059), hyaluronic acid sodium salt from *Streptococcus equi* (Catalog number: 40583, MW: 8,000 – 15,000) and (Catalog number: 96144 MW: 70,000 – 120,000), poly(vinyl alcohol) (Catalog number: 363138, MW: 31,000-50,000, 96-99% hydrolyzed) and (Catalog number: 363065, MW: 146,000-186,000 99+% hydrolyzed), streptavidin from *Streptomyces avidinii*, and DTT (OmniPur® Grade ≥ 99.4%) from Sigma-Aldrich (St. Louis, MO). We purchased dextran from *Leuconostoc mesenteroides* (Catalog number: J62775, MW: 6,000) from Alfa Aesar (Ward Hill, MA). We purchased chloroform (ACS

grade, purity ≥ 99.8%, with 0.75% ethanol as preservative), 96% ethanol (molecular biology grade), 200 proof ethanol (molecular biology grade), acetone (ACS grade), and Invitrogen 10× phosphate buffered saline (PBS) (pH 7.4, 0.2 μm filtered, 1.37 M sodium chloride, 0.027 M potassium chloride, 0.080 sodium phosphate dibasic, 0.020 M potassium phosphate monobasic) from Thermo Fisher Scientific (Waltham, MA). We obtained 18.2 MΩ Type I ultrapure water from a Milli-Q® IQ 7000 Ultrapure Lab Water System (Burlington, MA). We purchased 1,2- dioleoyl-*sn*-glycero-3-phosphocholine (18:1 (Δ9-cis) PC (DOPC)), 23-(dipyrrometheneboron difluoride)-24-norcholesterol (TopFluor™ Chol), cholesterol (ovine wool, >98%), 1,2-dipalmitoyl-*sn*-glycero-3-phosphocholine (16:0 PC (DPPC)), 1,2-dioleoyl-*sn*-glycero-3-phosphoethanolamine-N-(lissamine rhodamine B sulfonyl) (ammonium salt) (Rhod-DOPE), 1,2-distearoyl-*sn*-glycero-3-phosphoethanolamine-N-[biotinyl(polyethylene glycol)-2000] (ammonium salt) (PEG2000-Biotin-DSPE)and 1,2-distearoyl-*sn*-glycero-3-phosphoethanolamine-N-[methoxy(polyethylene glycol)-2000](ammonium salt) (PEG2000-DSPE) from Avanti Polar Lipids, Inc. (Alabaster, AL). We purchased a myTXTL Pro Cell-Free Expression Kit from Daicel Arbor Biosciences (Ann Arbor, MI). We purchased actin (> 99% pure, rabbit skeletal muscle), actin: HiLyte™ Fluor 488 Labelled (>99 % pure, rabbit skeletal muscle) fascin-1 (wild-type, human-recombinant), actin polymerization buffer (10× stock), and general actin buffer (1× stock) from Cytoskeleton, Inc. (Denver, Co).

Procedure for cleaning glass slides and nanocellulose paper

We clean eight 25 mm × 75 mm glass slides by sonicating in a Coplin staining jar sequentially for 10 minutes each in acetone, 200 proof ethanol, and Type I ultrapure water.[2] We dry the slides under a stream of nitrogen and place the slides in a 65 °C oven for 2 hours.

We cut a single 483 mm × 610 mm (19 in × 24 in) sheet of nanocellulose paper into 1/8th sections and place the sections in 250 mL of 96 % molecular biology grade ethanol in a glass crystallizing dish (45 mL, dish diameter × height 40 mm × 25 mm) for 15 minutes. The liquid in the dish was manually agitated occasionally. After 15 minutes the ethanol was discarded and the process repeated once. 250 mL of Type I ultrapure water was then added to the dish, swirled three times, and then discarded. This process was repeated an additional three times. Then 250 mL of Type I ultrapure water was added to the dish and allowed to soak for a further 15 minutes with occasional manual agitation. The water was then discarded, and the process was repeated once. Then the individual paper sections were removed and placed on an aluminum foil. We then placed another piece of aluminum foil loosely on top of the foil to prevent dust particles from settling on the wet paper sheets. We placed the foil with wet paper in a 65 °C oven overnight. The next day we remove the paper and store it in a closed 150 mm diameter polystyrene Petri dish on a lab bench until further use.

Preparation of polymer solutions

The concentration of polymer solutions, the temperature, the method of agitation, and the approximate time for dissolution are shown in Table S7. We weigh the mass of polymer using an analytical balance. We then dissolve the polymer in Type I ultrapure water in a 2 mL PCR tube or a 15 mL conical centrifuge tube depending on the volume of polymer solution we needed. We prepare 1 mL (hyaluronic acid, poly-D-lysine, salmon DNA, BSA) or 10 mL (agarose, PVA, dextran, carrageenan) of polymer solution. Agarose, PVA, and carrageenan were heated using a dry heating block (Thermo Scientific Multi-Blok Heater) set at the desired temperature to aid dissolution (Table S7). For experiments to determine the optimal polymer-NSC, the polymer solutions were diluted with isotemperature Type I ultrapure water. For the fabrication of large

pieces PCP, the polymer solutions were prepared at the concentration needed to obtain the desired polymer-NSC, for example, 0.3 % w/w for ULGT agarose and 4.85 % w/w for dextran. Polymer solutions were applied immediately at the preparation temperature onto paper preheated to 40 ° C. We prepare fresh polymer solutions each time we prepare paper.

Fabrication of PCP and PCG substrates

We place the cleaned glass slides on a Parafilm piece on a hotplate set at 40 °C and deposit the polymer solution using a micropipette (e.g. 1,162 µL of the ULGT agarose solution at various % w/w). We spread the solution evenly with the side of a 1000 µL pipette tip. The glass slides were left on the hotplate for 4 hours to dry. The PCG substrates were stored face up in a clean Petri dish and used within 24 hours.

We prepare PCPs of different sizes. We cut the cleaned nanocellulose paper to 22 mm × 22 mm squares when using relatively expensive polymers or when we planned to do a limited number of experiments. We place the pieces of paper on a piece of Parafilm on a hotplate set at 40 °C. We then apply 300 µL of the polymers at various % w/w on the substrates. The polymer solution was evenly spread on the substrates with the side of a 1000 µL pipette tip. We coat a whole strip of the cleaned 76 mm × 114 mm paper when we perform multiple experiments and when we store the paper. We apply 5.4 mL of warm 0.3 % w/w ULGT agarose solution using a 1000 µL micropipette in a serpentine pattern across the length of the paper. Then, the 60 mm section of an L-shaped glass delivery tube (180 mm × 60 mm) was passed four times back and forth along the 114 mm length of the paper to spread the solution evenly, careful not to allow any polymer solution to spill over the sides of the paper. The substrates were left on the hotplate for 4 hours. PCP was stored face up in a clean Petri dish.

Commonly available lab hot plates could not accommodate the 279 mm × 178 mm (11-in. × 7-in). piece of nanocellulose paper for the experiments with the baking tray. We thus place a sheet of aluminum foil as a backing on a baking tray followed by the nanocellulose paper. To obtain a polymer-NSC of 4.3 nmol/cm^2, we deposit a total of 4.25 mL of a 4.85 % w/w solution of dextran onto the paper. Using a bulb and glass Pasteur pipette, we deposited 3 mL of the solution onto the paper in a serpentine pattern on the left 2/3rd of the paper along the 178 mm width. The 180 mm handle of the L-shaped glass delivery tube was moved up and down once in a smooth controlled motion to spread the dextran solution evenly. We next apply 1.25 mL of the dextran solution onto the right 1/3rd of the paper in a straight line. We complete the coating process by moving the 60 mm side of the glass delivery tube up and down once along the 178 mm width. We then placed the baking tray with the wet paper in an oven set to 40 °C to dry for 4 hours.

Buffers

All hydration and sedimentation buffers are made as needed from stock solutions of 1 M sucrose, 1 M glucose, and 10 × PBS and used within 1 hour. 1 M sucrose and glucose stock solutions were stored in a 4 °C fridge and used for a maximum of two weeks. If solutions are used past this time, we find that the yield of the controls had a high likelihood of being low. Occasionally, even when all protocols are followed the yield falls. In these cases, remaking the buffers and performing the controls restore yields. We use 150 µL of 1× PBS + 100 mM sucrose as the hydration buffer for PCP-assisted hydration performed at 4 ºC, 22 ºC, 37 ºC for 1 hour and at 45 ºC performed for 20 minutes. We use 160 µL 0.97× PBS + 97 mM sucrose as the hydration buffer for PCP-assisted hydration performed at 45 ºC for 1 hour to account for the 10 µL of buffer that evaporates. All buffers were warmed to the desired temperature for 1 hour using a dry heating block (Multi-Blok

Heater, Thermo Scientific) or chilled to the desired temperature in an Isotemp™ low temperature incubator (model number: 3724, Fisher Scientific, Waltham, MA) before use.

Deposition of lipids

We deposit lipids as described previously.[1,20] We cut circular disks of the PCP using a circle hole punch (EK Tools Circle Punch, 3/8 in.). We deposited 10 μL of the lipid solution onto the polymer-coated side of the PCP evenly using a glass syringe (Hamilton) while holding the paper with clean metal forceps. The lipid-coated PCP disks were placed on a clean glass slide and into a standard laboratory vacuum desiccator for 1 hour to remove traces of organic solvent prior to hydration.

Procedure for PCP-assisted hydration and PCG-assisted hydration

We perform PCG-assisted hydration as previously described.[2] We perform PCP-assisted hydration as previously described for the PAPYRUS technique with minor modifications.[1,20] 48-well plates were warmed on a hotplate or chilled in a low temperature incubator for 1 hour if hydration was not performed at room temperature. Then, the lipid-coated PCP was placed into the wells of the 48-well plate and allowed to equilibrate for 5 minutes. Next, we add the isotemperature hydration buffer to the wells and allow the samples to hydrate for 1 hour. For experiments probing the effect of incubation time, we changed the incubation time to 20 mins, 2 hours, or 24 hours.

Procedure for harvesting the GUVs

We harvest GUVs from the substrates as previously described at the temperature of assembly.[2] We pipette 100 μL of the hydrating solution with a cut 1000 μL pipet tip on 6 different regions of the PCP to cover the whole area. On the 7th time, we aspirate all the GUV containing solution and transfer the liquid into a 0.5-mL PCR tube.

Control procedures

We normalize the concentration of the lipid solution that we prepare to control batch-to-batch variations of the mass of DOPC powder obtained from the manufacturer. We prepare GUVs using 10 μL of a nominal 1.0 mg/mL of DOPC:TopFluor™ Chol 99.5:0.5 using the standardized PAPYRUS procedure[1,3] using freshly prepared buffers and clean nanocellulose paper. We measure the molar yield and the distribution of diameters. If the yield was below 33 ± 2 %, we infer that the mass of DOPC was different from the stated nominal mass. To correct this difference, we perform the PAPYRUS technique by applying 10 μL of the lipid solution at a nominal concentration of 0.8 mg/mL, 1.0 mg/mL, and 1.2 mg/mL. We calculate the molar yield assuming an applied lipid amount of 10 μg. We renumber the concentration of the lipid solution that resulted in a yield closest to a range of 32 ± 2 % as 1 mg/mL. We find that approximately 1 in 10 DOPC lipid vials from the manufacturer had an apparent lipid mass that was sufficiently different to require this correction.

To minimize technique-dependent variability, we ensure that the experimentalist can perform the PAPYRUS technique three independent times on three separate days and obtain a molar yield of 33 ± 2 % and a distribution of sizes similar to those previously published. Reproducing previously published results serves as a check for the experimentalist's skill and care before trying new conditions with unknown yields. Lower than expected yields with validated lipid and buffers were often due to incorrect lipid deposition technique (allowing the lipid to coat the underside of the paper, for example) or poor harvesting technique.

Quantification of GUV yields

Imagining of the harvested free-floating GUVs was conducted as previously described.[3] We construct imaging chambers by placing poly(dimethylsiloxane) (PDMS) chambers with dimensions of 5.9 mm × 5.9 mm × 1 mm (length × width × height) on glass microscope slides. We

passivate the chamber with 1 mg/mL casein in PBS to prevent the rupture of GUVs on the surface of bare glass. We thoroughly rinse the chambers with ultrapure water after passivation by gently pouring 50 mL of water from a 50 mL Falcon tube over the chambers three times. We measure the osmolarity of a 20 μL aliquot of the GUV suspension and a 20 μL aliquot of our standard sedimentation buffer, 1×PBS + 100 mM glucose, using a freezing point depression multi-sample osmometer (Model 2020, Advanced Instruments, USA). The standard sedimentation buffer served as an internal control. The osmolarity of the GUV suspension varied slightly from sample-to-sample due to the dissolution of the polymer. Osmotic pressure of the GUV solution can range from 368 mOsm/kg H_2O to 438 mOsm/kg H_2O. The osmolarity of the standard sedimentation buffer was 375 mOsm/kg H_2O. We adjust the concentration of the glucose to ensure that the sedimentation buffer was isoosmolar with the GUV suspension. We fill the passivated chamber with 58 μL of the isoosmolar sedimentation buffer. We pipette 2 μL aliquot of the harvested GUV suspension in the middle of the chamber, aspirate 2 μL of the solution and deposit in the middle of four quadrants and then the mid-section of the chamber to ensure even distribution of the GUVs. We cover the sedimentation chambers with a glass coverslip and allow the GUVs to sediment for 3 hours in a covered 150 mm Petri dish with a moistened Kimwipe to minimize evaporation. We use an upright confocal laser-scanning microscope (LSM 880, Axio Imager.Z2m, Zeiss, Germany) with a 10× Plan-Apochromat objective with a numerical aperture of 0.45 to capture images. We image using an automated tile scan and autofocus routine (49 images, 5951.35 μm × 5951.35 μm, (3212 pixels × 3212 pixels) to capture the entire area of the chamber. For vesicles labeled with TopFluor™ Chol, we use a 488 nm argon laser. We set the pinhole to 15.16 Airy units which gave a confocal slice thickness of 79.3 μm. For phase-separated vesicles we capture dual-channel images. We use a 488 nm argon laser and a 561 nm diode-pumped solid-state laser. We image

using the line-switching scanning mode. We set the pinhole of the rhodamine channel to be 14.57 Airy units which gives a confocal slice thickness of 79.4 μm. We set the pinhole of the TopFluor™ Chol channel to be 17.76 Airy units which gives a confocal slice thickness of 79.4 μm. We normalize the laser power by measuring the intensity of 10 vesicles with diameters between 9 and 11 μm from 3 images using the line tool in FIJI. We adjust the laser power so that the intensity was within a range of 59 ± 3 arbitrary intensity units.

Determination of optimal polymer-NSC

To determine the optimal polymer-NSC we image the configuration of the film after 1 hour of hydration. We typically prepare 6 samples by depositing 300 μL of 0.1, 0.3, 0.5, 0.7 and 1.0 % w/w of polymer on a 22 × 22 mm square of paper. We use an upright confocal laser-scanning microscope (LSM 700 Axio Imager.Z2m, Zeiss, Germany) with a 10× Plan-Apochromat objective with a numerical aperture of 0.45 to examine and capture images. In general, surfaces with polymer-NSCs that have only lipid bilayer stacks and with minimal buds will not have high yields. These polymer-NSCs are not considered further. For surfaces that have apparent buds, the buds are examined for evidence of dewetting patterns to distinguish GUV buds from pseudobuds. Surfaces that show low amount of pseudobuds and high number of GUV buds are chosen as having the optimal polymer-NSC. On some surfaces, determining which of the two surfaces with adjacent polymer-NSCs had a higher number of buds instead of pseudobuds was challenging. For these surfaces, the buds are harvested, the molar yield of GUVs is measured, and the higher yielding surface is considered to have the optimal polymer-NSC. Only the yield at the optimal polymer-NSC is reported in Table 1. Additional yields that we measured are provided in Table S2-S5, for completeness.

For the images in Figure 2 we use a 20× Plan-Apochromat objective with a numerical aperture of 1.0. We capture a Z-stack (135 images, 151.8 μm × 151.8 μm, 1272 pixels × 1272 pixels, slice thickness 1.5 μm, slice interval 0.745 μm) of a region that was representative of the surface and image from the surface of the substrate to 99.87 μm above the surface.

myTXTL expression of eGFP

We deposit 10 μg of lipid on a 9.5 mm diameter disc of PCP. We place the lipid coated PCP in a standard laboratory desiccator to remove traces of organic solvent. We use a circular hole punch (AIEX, 3mm diameter), to punch out two 3 mm disks. We punch the circular disk with the lipid coated side facing down ensuring that the lipid does not transfer to the punch. We use one 3 mm disk of lipid-coated PCP per PCR tube for a total of two samples. We prechill the 0.5-mL PCR tube in a 4 °C incubator for 1 hour before placing the lipid-coated PCP face up into the tube. We allow the paper to incubate for a further 5 minutes in the 4 °C incubator. Working on ice, we mix 12 μL of the myTXTL mix as described in the myTXTL manual.[44] We place the mixture on top of the paper, close the tube, and incubate for 1 hour at 4 °C to prevent premature expression. While still working in the incubator, we harvest by pipetting 10 μL of the hydrating solution with a cut 100 μL pipet tip 6× on the PCP to cover the whole area. We remove the tubes from the incubator and pool the two samples together in one 2 mL Eppendorf tube. We allow the tube to sit for 5 minutes to come to room temperature and add 80 μL of room temperature 2.8× PBS for a total volume of ~100 μL. This concentration of PBS was isomolar to the myTXTL mixture (~845 mOsm/kg) which ensured osmotic balance of the GUVs. We centrifuge the pooled samples for 60 minutes at 100×g in a swing bucket clinical centrifuge (AccuSpin 8c) equipped with 3D printed adapters for 2 mL Eppendorf tubes. We then remove 80 μL of the supernatant and resuspend the pelleted GUVs in the remaining solution by pipetting 6 times. We place the suspension in a 3.5

mm circular PDMS imaging chamber, place a coverslip, and incubate at room temperature (22 °C) for 6 hours. For the negative control, we followed the same protocol but omitted the T7 deGFP control plasmid from the reaction mixture.

myTXTL expression imaging and image processing

We obtain confocal images of the GUVs using an upright confocal laser-scanning microscope (LSM 880, Axio Imager.Z2m, Zeiss, Germany) with a 20× Plan-Apochromat objective with a numerical aperture of 1.0. We capture images with an area of 212.55 µm × 212.55 µm, (1784 pixels × 1784 pixels) using a pinhole of 1.51 A.U. for the 488 nm channel (collecting emissions from 494 nm to 555 nm) and 1.24 A.U. for the 561 nm channel (collecting emissions from 570 nm to 709 nm). We measured the fluorescence intensity of the lumen of all the GUVs from 1 image per sample using FIJI. We draw circular ROIs wholly within the dark lumen of the GUVs and avoid selecting the bright pixels that correspond to the membrane. We ignore out of focus GUVs and bright objects which are not GUVs. For the negative control, we measured the intensity of GUVs in 5 images to get ~500 GUVs. We estimate the total number of GUVs in the chamber by dividing the number of GUVs in an image and multiplying with the total area of the chamber.

Actin encapsulation

We deposit 10 µg of DOPC:PEG2000-DSPE:PEG2000-Biotin-DSPE:Rhod-DOPE 95.9:3:1:0.1 mol %. on a 9.5 mm diameter disc of PCP. We place the lipid-coated PCP in a standard laboratory desiccator to remove traces of organic solvent. We use a circular hole punch (AIEX, 3 mm diameter), to punch out three 3 mm disks of lipid-coated PCP. We punch the circular disk with the lipid-coated side facing down ensuring that the lipid does not transfer to the punch. We use one 3 mm disk per PCR tube for a total of three samples. To minimize temperature gradients that can hasten the polymerization of actin, we then work in a 4°C cold room for the duration of the

hydration step. We place the PCR tubes containing the lipid coated-PCP on a laboratory bench in the cold room for at least 5 minutes to allow them to reach 4 °C. Working on ice, we prepare actin mix consisting of 90:10 actin: HiLyte™ Fluor 488 actin, fascin, DTT, and sucrose in general actin buffer. We then add the actin polymerization buffer and pipette 6 times to mix thoroughly. We quickly aspirate the well-mixed mixture and add 12 μL to each lipid-coated PCP disk in the PCR tubes. The final concentration of the mix shown in Figure 4 is 12 μM actin, 1.8 μM fascin, 1 mM DTT, 300 mM sucrose, 1× general actin buffer and 1× polymerization buffer. We wrap the PCR tubes with aluminum foil and allow the samples to incubate for 1 hour at 4 °C. We harvest by pipetting 10 μL of the hydrating solution with a cut 100 μL pipet tip 6 times on the PCP to cover the whole area. We pool the three samples together in one 2 mL Eppendorf tube and add 200 μL of isomolar sedimentation buffer made of 1× general actin buffer, 1× actin polymerization buffer, 1 mM DTT and 300 mM glucose for a total volume of ~230 μL. We centrifuge the pooled samples for 20 minutes at 100×g in a swing bucket clinical centrifuge (AccuSpin 8c) equipped with 3D printed adapters for 2 mL Eppendorf tubes. We then remove 210 μL of the supernatant and resuspend the pelleted GUVs in the remaining 20 μL of buffer by pipetting gently 6 times.

Actin imaging and image processing

GUVs imaged on the Zeiss LSM880 were not bound to the glass coverslip. We add 20 μL of the GUV suspension into a circular 3.5 mm diameter PDMS chamber and cover the chamber with a coverslip. We imaged the sample after 3 hours. We found locations with multiple GUVs and image confocal Z-stacks with a 20× Plan-Apochromat objective with a numerical aperture of 1.0 starting from the surface of the glass slide to 2 slices above the GUV that was furthest away from the surface. We use a pinhole of 1.01 A.U. for the 488 nm channel (slice thickness 1.33 μm, slice interval 0.667 μm, collecting emissions from 494 nm to 555 nm) and 0.83 A.U and for the 561

nm channel (slice thickness 1.4 μm, slice interval 0.667 μm, collecting emissions from 570 nm to 709 nm). The image size was 592 × 592 pixels. GUVs imaged on the Nikon Ti2-E were bound to the coverslip through biotin-streptavidin linkers. For bound GUVs, we prepare biotin functionalized coverslips as previously described.[45] We place 3.5 mm circular PDMS chambers on the functionalized coverslips and allow 10 μL of 0.1 mg/mL streptavidin to incubate in the chamber for 15 minutes. We then wash the chamber 6 times with 1× PBS, then 2 times with the sedimentation buffer. We add 20 μL of the GUV suspension into the chamber and allow the GUVs to sediment for 3 hours in a closed 150 mm Petri dish with a reservoir of water to prevent evaporation. We then remove unbound GUVs by removing 10 μL of the solution from the top of the sedimentation chamber, careful not to contact the surface of the coverslip. We then add 10 μL of sedimentation buffer and seal the chamber with a glass slide. We imaged the sample after 3 hours. We use an inverted microscope (Nikon Ti2-E with AxR point scanning confocal) equipped with an NSPARC detector, a CFI Plan Apo Lambda S 60XC Silicone Immersion Objective with a numerical aperture of 1.3 to capture confocal Z-stacks. We capture confocal Z-stacks from the surface to 2 slices above the highest GUV using a pinhole of 2 A.U. The images were 2048 pixels × 2048 pixels with a slice interval 0.316 μm.

Image processing was performed using FIJI. We analyzed GUVs > 6.5 μm. GUVs were binned based on the diameter with GUVs edges of 0.5 μm below and 0.5 μm above the nearest whole number. We identified bundles in the GUV lumens manually. When the GUVs were not bound to the coverslip, it was difficult to discern whether the actin bundles were forming single actin rings, single actin rings with breaks or branches, or multiple actin rings. Therefore, we do not separate the actin bundle conformation into categories for this sample. For the superresolution images, GUVs with a single actin bundle that appeared to completely encircle the membrane of

the GUV were classified as “single actin rings”, GUVs with a single actin bundle that encircled the membrane of the GUV but had gaps or with a single actin bundle that encircled the membrane of the GUV but had one or more branches were classified as “single actin rings that were not closed or had one or more branches” and GUVs with multiple actin bundles that encircled the membrane of the GUVs were classified as “multiple actin rings”. We estimate the total number of GUVs in the chamber by dividing the number of GUVs in an image and multiplying with the total area of the chamber.

Large scale-assembly of GUVs using PCP-assisted hydration

We adapt the procedure for reported in reference [3] with modifications. The lipid solution consisted of DOPC: PEG2000-DSPE: TopFluor™ Chol at 96.5:3:0.5 mol % dissolved in chloroform at a concentration of 3.5 mg/mL. Working in a chemical safety hood, we deposit 2 mL of the lipid solution using the L-shaped glass delivery tube similar to how the dextran solution was coated onto the paper. The lipid-coated PCP was placed into a standard laboratory vacuum chamber for 1 hour to remove traces of organic solvent. We then place the lipid-coated PCP in a 330 mm × 279 mm (13-in. × 11-in.) baking tray (inner dimension, 290 mm × 188 mm (11.4-in × 7.4-in)) with PTFE magnetic stir bars placed on the corners of the paper to prevent curling of the paper upon hydration. The paper was hydrated with 200 mL of 1× PBS + 100 mM sucrose. We incubate the sample for 1 hour before removing the stir bars. We harvest the GUVs using a flexible shrink film (Grafix art) cut to a dimension of 188 mm × 127 mm (7.4-in. × 5-in). We move the film across the 279 mm (11-in.) edge of the PCP while applying gentle pressure to detach the GUV buds from the surface. We repeat the process a second time. We transfer the solution containing the GUVs into four 50 mL Falcon tubes for storage. Quantification of GUV yield was performed similarly to samples prepared in 48-well plates.

Preparation of a tissue-like close-packed layer of GUVs

To obtain the image shown in Figure 5b, we mix 7.5 mL of the sample with 7.5 mL of 1×PBS+100 mM glucose in a 15 mL Falcon tube and centrifuge at 2080× g for 30 minutes to pellet the GUVs. We then remove 14 mL of the supernatant. Next, using a micropipette, we take a 10 μL aliquot from the bottom of the remaining 1 mL and mix the aliquot with 50 μL of 1× PBS+100 mM glucose and place the suspension into an imaging chamber. We allowed the GUVs to sediment for 3 hours before imaging. We acquired confocal Z-stacks starting from the bottom of the chamber and extending to a height of 35.8 μm (47 slices, 425.1 μm × 425.1 μm, 3568 pixels × 3568 pixels, with a slice thickness of 1.52 μm and slice interval 0.762 μm) using a 20× 1.0 NA Plan-Apochromat objective with a pinhole of 1.02 A.U.

Characterizing the long-term functionality of PCP

Two separate pieces of ULGT agarose PCP were stored at 4 °C and 22 °C in 150 mm polystyrene Petri dishes. We assemble GUVs from both stored pieces of ULGT agarose PCP and measure the molar yields at 1, 4, 7, 14, 21 and 28 days. We additionally assemble GUVs from a piece of ULGT agarose PCP stored at 4 °C for 28 days without removing it from the low temperature incubator.

Author contributions

A.B.S. conceived and directed the study. A.C. performed experiments and analyzed the data. V.V. performed the scale up experiments. J.P. performed preliminary experiments. A.B.S and A.C. wrote the manuscript. All authors have given approval to the final version of the manuscript.

Data availability

The data supporting this article have been included in the manuscript.

Conflicts of interest

There are no conflicts to declare.

Acknowledgements

This work was funded by the National Science Foundation through NSF CAREER DMR-1848573. The data in this work was collected, in part, with a confocal microscope acquired through the National Science Foundation MRI Award Number DMR-1625733, and a scanning electron microscope acquired through NASA Grant NNX15AQ01A that are housed and managed by the Imaging and Microscopy Core at UC Merced. We would like to thank Brad Bartholomai Ph.D. and our local team from Nikon Instruments for their assistance in obtaining the superresolution images of actin in GUVs. The schematic in figure 4 was created in BioRender. Cooper, A. (2025) https://BioRender.com/g69f517.

References

[1] J. Pazzi, A. B. Subramaniam, *J Colloid Interface Sci* **2024**, *661*, 1033.
[2] A. Cooper, A. B. Subramaniam, *Soft Matter* **2024**, *20*, 9547.
[3] J. Pazzi, A. B. Subramaniam, *ACS Appl Mater Interfaces* **2020**, *12*, 56549.
[4] X. Zhang, C. Li, F. Liu, W. Mu, Y. Ren, B. Yang, X. Han, *Nat Commun* **2022**, *13*, DOI 10.1038/s41467-022-29571-3.
[5] J. Wu, Y. Wei, J. Lan, X. Hu, F. Gao, X. Zhang, Z. Gao, Q. Liu, Z. Sun, R. Chen, H. Zhao, K. Fan, X. Yan, J. Zhuang, X. Huang, *Small* **2022**, *18*, 2202145.
[6] A. Witkowska, L. Jablonski, R. Jahn, *Scientific Reports 2018 8:1* **2018**, *8*, 1.
[7] R. Cao, D. Kumar, A. D. Dinsmore, *Langmuir* **2021**, *37*, 1714.
[8] J. C. Stachowiak, C. C. Hayden, D. Y. Sasaki, *Proc Natl Acad Sci U S A* **2010**, *107*, 7781.
[9] W. C. Su, J. C. S. Ho, D. L. Gettel, A. T. Rowland, C. D. Keating, A. N. Parikh, *Nature Chemistry 2023 16:1* **2023**, *16*, 54.
[10] F. C. Tsai, G. H. Koenderink, *Soft Matter* **2015**, *11*, 8834.
[11] Y. Bashirzadeh, H. Moghimianavval, A. P. Liu, *iScience* **2022**, *25*, 104236.
[12] T. Litschel, C. F. Kelley, D. Holz, M. Adeli Koudehi, S. K. Vogel, L. Burbaum, N. Mizuno, D. Vavylonis, P. Schwille, *Nat Commun* **2021**, *12*, DOI 10.1038/s41467-021-22422-7.
[13] G. Chen, R. Levin, S. Landau, M. Kaduri, O. Adir, I. Ianovici, N. Krinsky, O. Doppelt-Flikshtain, J. Shklover, J. Shainsky-Roitman, S. Levenberg, A. Schroeder, *Proc Natl Acad Sci U S A* **2022**, *119*, e2207525119.
[14] D. Blanken, P. Van Nies, C. Danelon, *Phys Biol* **2019**, *16*, DOI 10.1088/1478-3975/ab0c62.
[15] K. Nishimura, S. Tsuru, H. Suzuki, T. Yomo, *ACS Synth Biol* **2015**, *4*, 566.
[16] D. T. Gonzales, N. Yandrapalli, T. Robinson, C. Zechner, T. Y. D. Tang, *ACS Synth Biol* **2022**, *11*, 205.
[17] T. Litschel, P. Schwille, *Annu Rev Biophys* **2021**, *50*, 525.
[18] K. S. Horger, D. J. Estes, R. Capone, M. Mayer, *J Am Chem Soc* **2009**, *131*, 1810.
[19] A. Weinberger, F. C. Tsai, G. H. Koenderink, T. F. Schmidt, R. Itri, W. Meier, T. Schmatko, A. Schröder, C. Marques, *Biophys J* **2013**, *105*, 154.
[20] A. Cooper, V. Girish, A. B. Subramaniam, *Langmuir* **2023**, *39*, 5579.
[21] B. A. Miller-Chou, J. L. Koenig, *Progress in Polymer Science (Oxford)* **2003**, *28*, 1223.
[22] K. De France, Z. Zeng, T. Wu, G. Nyström, K. De France, Z. Zeng, T. Wu, G. Nyström, *Advanced Materials* **2021**, *33*, 2000657.
[23] D. Trache, A. F. Tarchoun, M. Derradji, T. S. Hamidon, N. Masruchin, N. Brosse, M. H. Hussin, *Front Chem* **2020**, *8*, 535734.
[24] S. L. Veatch, S. L. Keller, *Biophys J* **2003**, *85*, 3074.
[25] M. G. Gutierrez, N. Malmstadt, *J Am Chem Soc* **2014**, *136*, 13530.
[26] H. M. J. Weakly, K. J. Wilson, G. J. Goetz, E. L. Pruitt, A. Li, L. Xu, S. L. Keller, *Biophys J* **2024**, *123*, 3452.
[27] O. S. Kumru, S. B. Joshi, D. E. Smith, C. R. Middaugh, T. Prusik, D. B. Volkin, *Biologicals* **2014**, *42*, 237.

[28] R. P. Welch, H. Lee, M. A. Luzuriaga, O. R. Brohlin, J. J. Gassensmith, *Bioconjug Chem* **2018**, *29*, 2867.
[29] D. Marsh, *Handbook of Lipid Bilayers*, CRC Press, **2013**.
[30] R. B. Lira, R. Dimova, K. A. Riske, *Biophys J* **2014**, *107*, 1609.
[31] T. P. T. Dao, M. Fauquignon, F. Fernandes, E. Ibarboure, A. Vax, M. Prieto, J. F. Le Meins, *Colloids Surf A Physicochem Eng Asp* **2017**, *533*, 347.
[32] E. Parigoris, D. L. Dunkelmann, A. Murphy, N. Wili, A. Kaech, C. Dumrese, N. Jimenez-Rojo, U. Silvan, *Sci Rep* **2020**, *10*, 1.
[33] N. L. Mora, J. S. Hansen, Y. Gao, A. A. Ronald, R. Kieltyka, N. Malmstadt, A. Kros, *Chemical Communications* **2014**, *50*, 1953.
[34] M. L. Vázquez-González, A. C. Calpena, Ò. Domènech, M. T. Montero, J. H. Borrell, *Colloids Surf B Biointerfaces* **2015**, *134*, 31.
[35] S. Vasvani, P. Kulkarni, D. Rawtani, *Int J Biol Macromol* **2020**, *151*, 1012.
[36] K. Wang, M. Liu, R. Mo, *Med Drug Discov* **2020**, *7*, 100031.
[37] T. Barrett, H. Kobayashi, M. Brechbiel, P. L. Choyke, *Eur J Radiol* **2006**, *60*, 353.
[38] G. Sun, J. J. Mao, *Nanomedicine* **2012**, *7*, 1771.
[39] S. G. Lévesque, R. M. Lim, M. S. Shoichet, *Biomaterials* **2005**, *26*, 7436.
[40] D. Mazia, G. Schatten, W. Sale, *Journal of Cell Biology* **1975**, *66*, 198.
[41] E.-M. Pacheco-Quito, R. Ruiz-Caro, M.-D. Veiga, *Mar Drugs* **2020**, *18*, 1.
[42] Y. M. Lim, H. J. Gwon, J. H. Choi, J. Shin, Y. C. Nho, S. I. Jeong, M. S. Chong, Y. M. Lee, I. K. Kwon, S. E. Kim, *Macromol Res* **2010**, *18*, 29.
[43] R. Yegappan, V. Selvaprithiviraj, S. Amirthalingam, R. Jayakumar, *Carbohydr Polym* **2018**, *198*, 385.
[44] Daciel Arbor Biosciences, *MyTXTL ® Pro Cell-Free Expression Kit Cell-Free Protein Expression System User Manual*, **2024**.
[45] A. Z. T. Li, A. LiWang, A. B. Subramaniam, *bioRxiv* **2024**, 2024.10.13.617916.

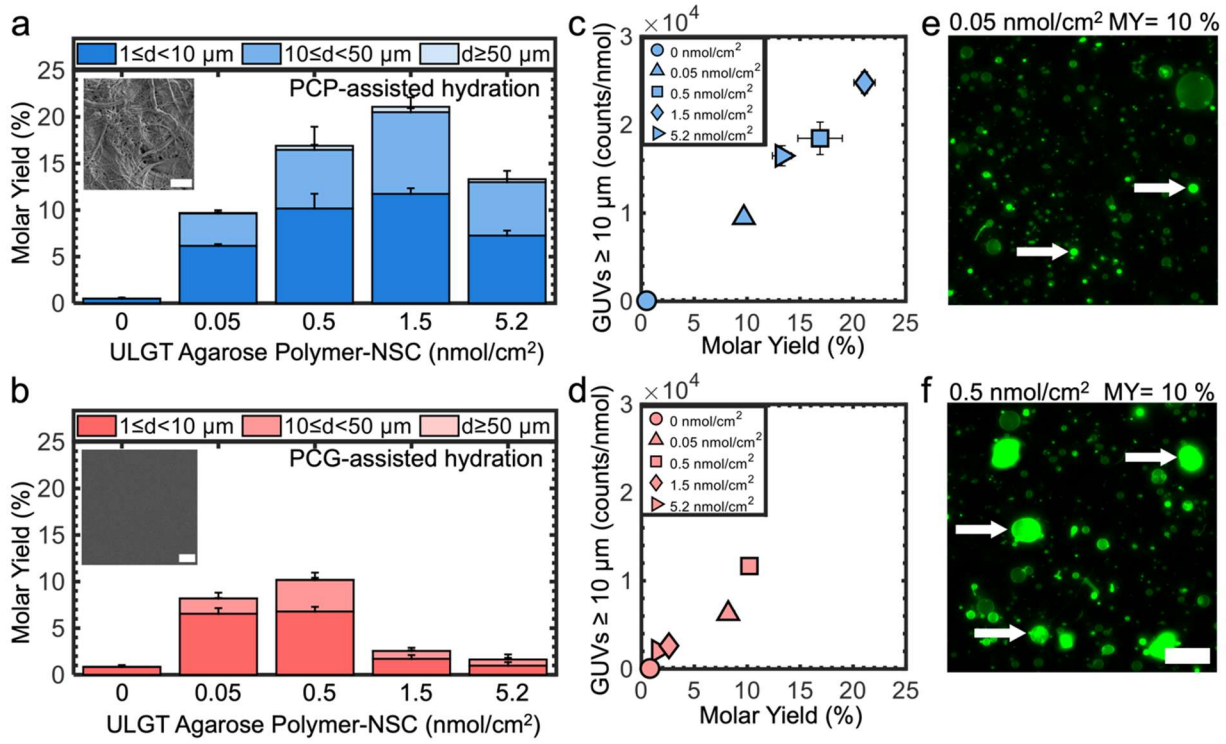

Figure 1. Yields of GUVs obtained using PCP- and PCG- assisted hydration at various ULGT agarose polymer-NSCs. a) Stacked bar plots of GUV yields from PCP-assisted hydration. The inset shows a SEM image of nanocellulose paper. b) Stacked bar plots of GUV yields from PCG-assisted hydration. The inset shows a SEM image of the glass slide. Each bar is split into 3 sections depending on the GUV diameter. The bar is an average of N=3 independent repeats. The error bars are one standard deviation from the mean. c) Scatter plot of the counts of GUVs with diameters ≥ 10 µm versus the total molar yield obtained using PCP-assisted hydration. d) Scatter plot of the counts of GUVs with diameter ≥ 10 µm versus the total molar yield obtained using PCG-assisted hydration. e,f) Representative single plane confocal microscopy images of harvested objects obtained from ULGT agarose-coated substrates with the same molar yield, 10 %. e) ULGT agarose PCP with a polymer-NSC of 0.05 nmol/cm^2. f) ULGT agarose PCG with a polymer-NSC of 0.5 nmol/cm^2 Scale bar a, b) 2 µm, f) 50 µm.

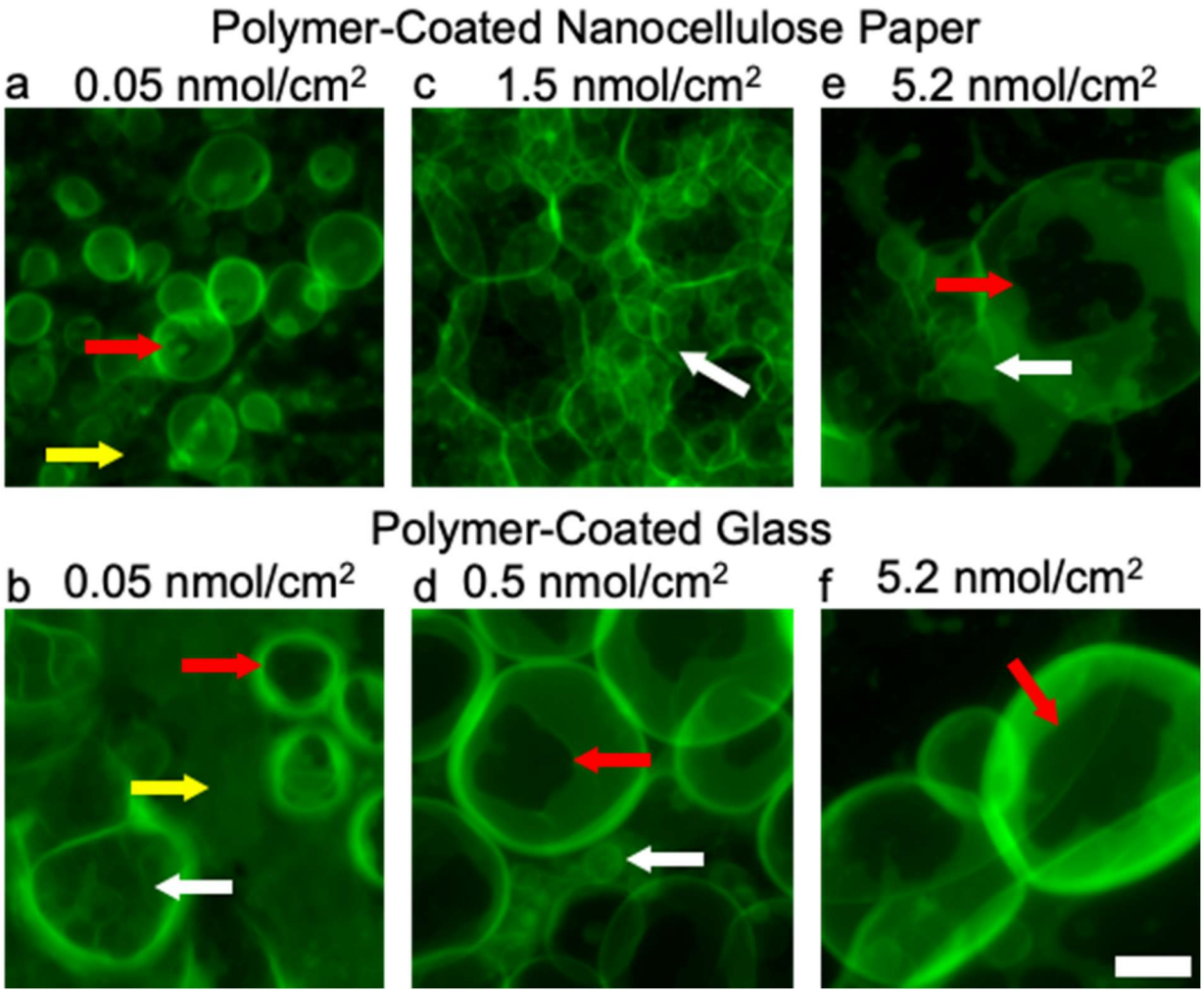

Figure 2. Surface morphology of DOPC films on ULGT agarose PCP and PCG. The images are two-dimensional projection of *z*-slices from 0 to 100 µm from the surface using the 'sum slices' algorithm. a) 0.05 nmol/cm^2 on nanocellulose paper, b) 0.05 nmol/cm^2 on glass slides, c) 1.5 nmol/cm^2 on nanocellulose paper, d) 0.5 nmol/cm^2 on glass slides, e) 5.2 nmol/cm^2 on nanocellulose paper, and f) 5.2 nmol/cm^2 on glass slides. The red arrows highlight examples of dewetting patterns in the pseudobuds. The white arrows highlight examples of GUV buds. The yellow arrows highlight examples of bilayer stacks. Scale bar is 10 µm.

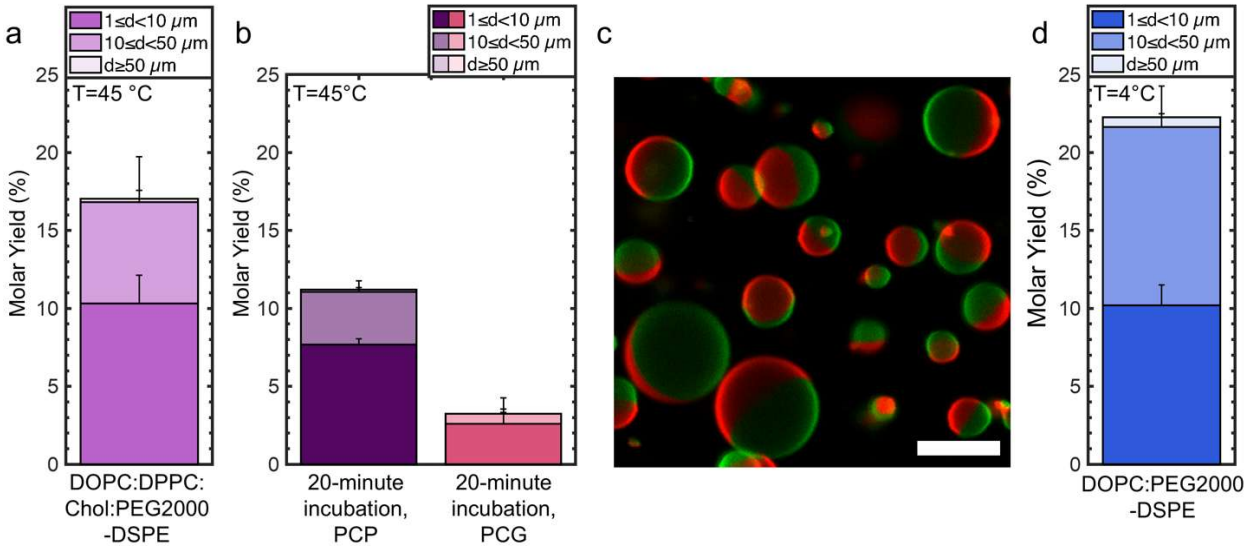

Figure 3. Molar yields of GUVs assembled at different temperatures using PCP- and PCG- assisted hydration. a) Molar yield of DOPC:DPPC:Chol:PEG2000-DSPE phase-separating GUVs obtained using PCP-assisted hydration after 1 hour of incubation at 45 °C. b) Molar yield of phase-separating GUVs obtained using PCP-assisted hydration and PCG- assisted hydration after 20 minutes of incubation at 45 °C. c) Representative image of the phase-separated GUVs at 22 ºC. d) Molar yield of DOPC:PEG2000-DSPE GUVs assembled at 4 °C using PCP-assisted hydration. Each bar is split into 3 sections that correspond to the GUV diameter range reported in the legend. Each bar is the average of N=3 independent repeats. The error bars are one standard deviation from the mean. Scale bar in c) is 50 µm.

Table 1 Polymer type, optimal polymer-NSC, lipid composition, and the resulting molar yields, GUV counts per μg of lipid, and percent non-GUV objects. Each value is reported as a mean ± standard deviation of N=3 independent repeats.

Polymer	Optimal Polymer-NSC (nmol/cm^2)	Lipid Composition	Molar Yield (%)	GUV Counts ($\times 10^5$ GUVs/μg)	Percent non-GUVs (%)
4°C					
Agarose, ULGT* 120 kDa	1.5	DOPC:PEG2000-DSPE	22.3 ± 2.0	5.4 ± 0.6	7.2 ± 0.3
Dextran, 100 kDa	1.9	DOPC:PEG2000-DSPE	17.7 ± 0.7	8.5 ± 0.8	10.1 ± 0.4
Hyaluronic Acid, 8-15 kDa	23	DOPC:PEG2000-DSPE	20.4 ± 0.9	10.8 ± 0.6	8.1 ± 0.2
Hyaluronic Acid, 70-120 kDa	2.7	DOPC:PEG2000-DSPE	12.6 ± 2.7	5.2 ± 1.6	9.8 ± 1.3
22 °C					
Agarose, ULGT* 120 kDa	1.5	DOPC:PEG2000-DSPE	21.1 ± 1.0	5.8 ± 0.5	8.3 ± 0.5
Bovine Serum Albumin	2.8	DOPC:PEG2000-DSPE	6.1 ± 0.5	3.4 ± 0.4	10.6 ± 0.7
Carrageenan, 521 kDa	1.2	DOPC:PEG2000-DSPE	16.4 ± 2.0	6.3 ± 1.2	7.0 ± 2.0
Dextran, 100 kDa	4.3	DOPC:PEG2000-DSPE	15.0 ± 0.3	5.8 ± 0.1	11.3 ± 0.1
DNA, Single stranded from salmon testes	2.3	DOPC:PEG2000-DSPE	6.7 ± 1.2	6.1 ± 1.4	9.7 ± 0.3
Hyaluronic Acid, 70-120 kDa	1.5	DOPC:PEG2000-DSPE	15.5 ± 2.0	5.2 ± 1.6	9.8 ± 1.3
Hyaluronic Acid, 8-15 kDa	23	DOPC:PEG2000-DSPE	22.0 ± 2.5	10.1 ± 0.7	10.8 ± 0.1
Poly-D-Lysine, 70-150 kDa	6.2	DOPC:PEG2000-DSPE	18.6 ± 3.0	6.8 ± 1.4	9.3 ± 1.9
45°C					
Agarose, ULGT* 120 kDa	1.5	DOPC:DPPC:Chol:PEG 2000-DSPE	17.0 ± 2.7	5.0 ± 1.0	7.0 ± 0.03
Hyaluronic Acid, 8-15 kDa	23	DOPC:DPPC:Chol:PEG 2000-DSPE	17.5 ± 2.2	8.4 ± 1.6	15.8 ± 1.1

* Data from ULGT agarose PCP-assisted hydration reproduced from Fig. 1 and 3 for ease of comparison

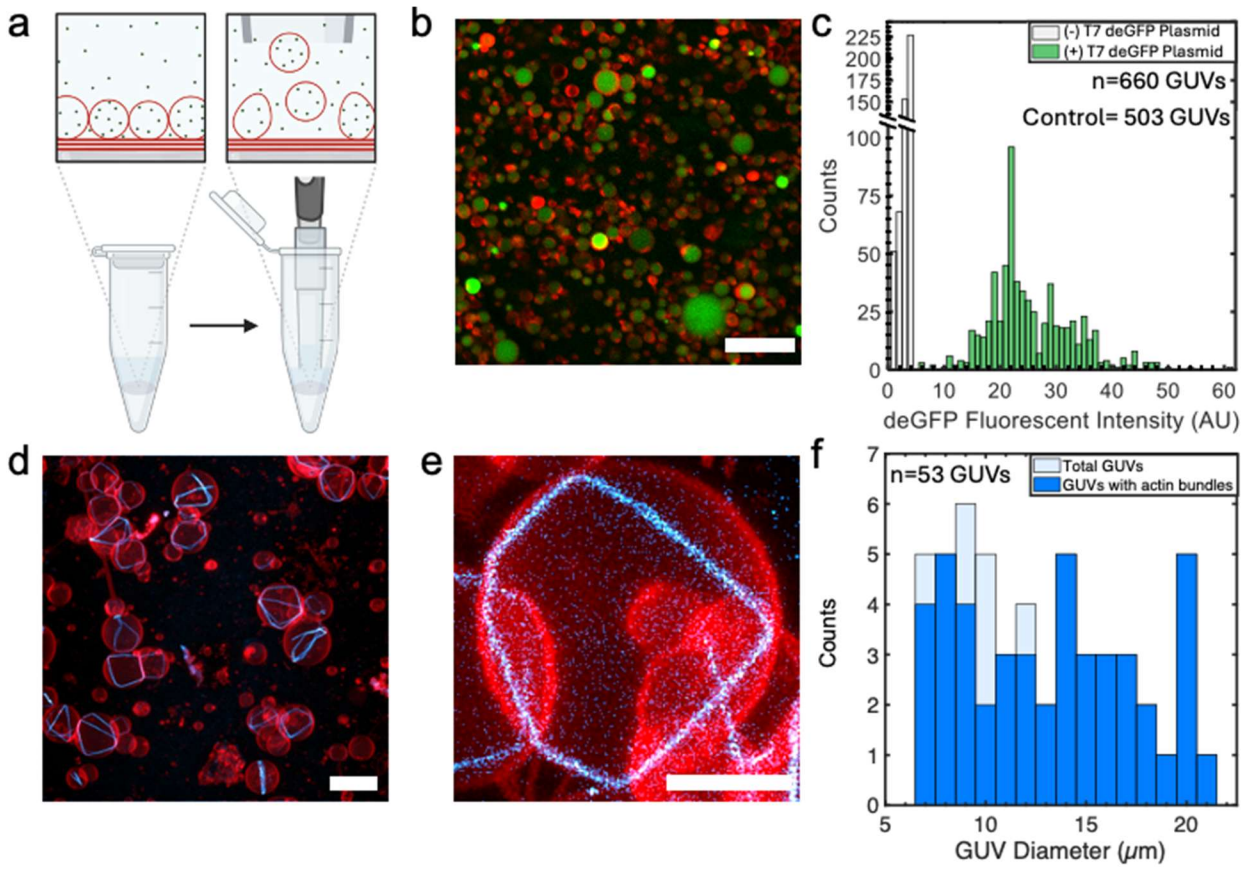

Figure 4. Encapsulation of complex biochemical mixtures using PCP-assisted hydration. a) Schematic of the encapsulation process of small volumes of precious mixtures in 0.5-mL PCR tubes. b) Representative two-channel image of GUVs encapsulating myTXTL cell free expression mixture with deGFP plasmid after 6 hours of incubation. The image is an overlay of the membrane channel, false colored red, and the deGFP channel, false colored green. c) Histogram of fluorescence intensities of deGFP in the lumens of GUVs that encapsulate myTXTL cell free expression mixture. The green bars show the distribution of luminal intensities with the deGFP plasmid, n=660 GUVs. The grey bars show the distribution of luminal intensities of a negative control that lacked the plasmid, n= 503 GUVs. d) Two-channel supperresolution image of multiple GUVs with actin rings in their lumens. The image is an overlay of the membrane channel, false colored red, and the actin channel, false colored cyan. e) A zoomed superresolution image of a

GUV with a single actin ring. f) Stacked bar plot of the counts of GUVs with actin rings vs the diameter of GUVs. n = 53 GUVs. Scale bars a,d) 20 µm, e) 2 µm.

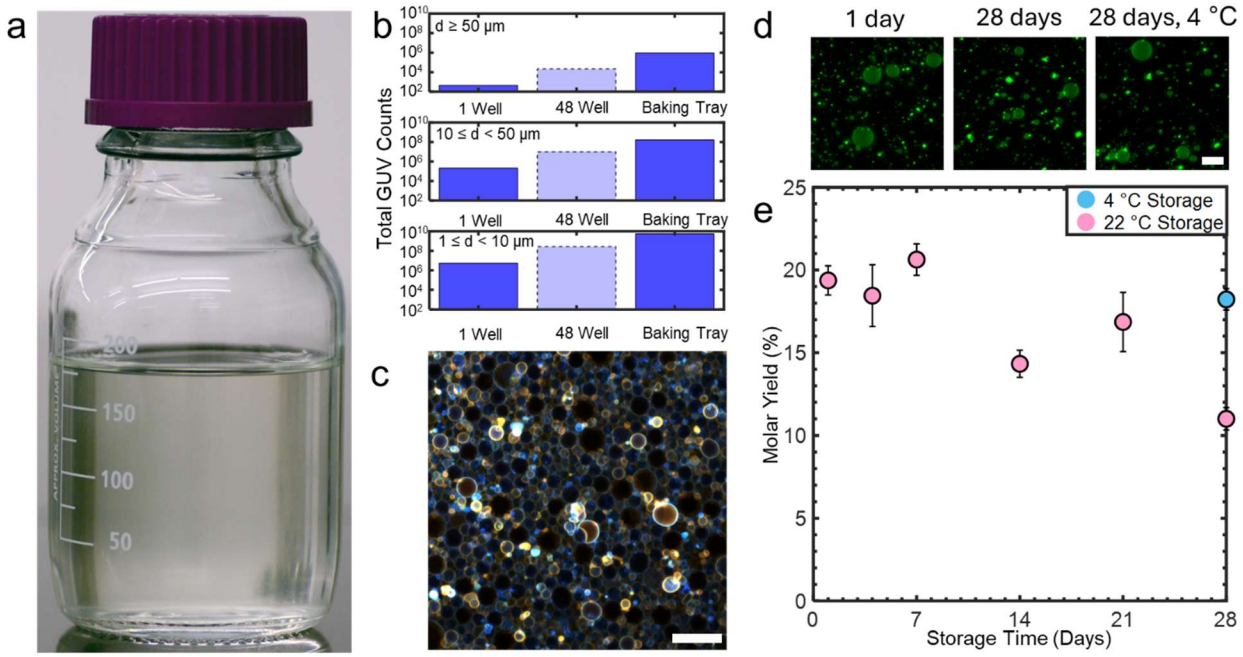

Figure 5. Versatility of PCP-assisted hydration. a) Photograph of a 188 mL suspension of GUVs in physiological saline obtained by performing PCP-assisted hydration using a 279 mm × 178 mm sheet of dextran PCP. The concentration of GUVs was 2.95×10^7 per mL for a total of 5.54×10^9 GUVs b) Bar plots of the total GUV counts from 1 well (dark blue bars with solid borders), hypothetical yield if using 48 wells (light blue bar with dashed borders), and from PCP-assisted hydration using the 279 mm × 178 mm dextran PCP (dark blue bars with solid borders). Note the logarithmic scale on the *y*-axis. Single well data is reproduced from Table 1. c) Z-coded projection of a tissue-like assembly of close-packed GUVs. d) Representative images of assembly from ULGT agarose PCP stored for 1 day and 28 days at 22 °C and for 28 days at 4 °C. e) Plot of the molar yield of GUVs obtained using stored ULGT agarose PCP. Scale bars are 50 µm.